NOVEL TECHNIQUE AND TECHNOLOGIES FOR ACTIVE OPTICAL REMOTE SENSING OF GREENHOUSE GASES

Upendra N. Singh

NASA Engineering and Safety Center
NASA Langley Research Center
Hampton, Virginia, USA
Upendra.n.singh@nasa.gov

Tamer F. Refaat and Mulugeta Petros

Remote Sensing Branch
NASA Langley Research Center
Hampton, Virginia, USA

Abstract— **The societal benefits of understanding climate change through identification of global carbon dioxide sources and sinks led to the desired NASA's active sensing of carbon dioxide emissions over nights, days, and seasons (ASCENDS) space-based missions of global carbon dioxide measurements. For more than 15 years, NASA Langley Research Center (LaRC) have developed several carbon dioxide active remote sensors using the differential absorption lidar (DIAL) technique operating at the two-micron wavelength. Currently, an airborne two-micron triple-pulse integrated path differential absorption (IPDA) lidar is under development. This IPDA lidar measures carbon dioxide as well as water vapor, the dominant interfering molecule on carbon dioxide remote sensing. Advancement of this triple-pulse IPDA lidar development is presented.**

Keywords—carbon dioxide; water vapor; triple-pulse laser; lidar; DIAL; IPDA

I. INTRODUCTION

The lack of spatially extensive, high-accuracy atmospheric CO_2 data limits the ability to construct accurate inverse estimates of the sources and sinks of the gas. ASCENDS study advocate an active CO_2 remote sensing mission to provide critical global CO_2 measurements [1]. Airborne full range-resolved DIAL measurements of CO_2 is beyond near-term technological capability. In absence of such capability airborne column dry-air volume mixing ratio of CO_2 (XCO2) measurements weighted toward the boundary layer (BL) are ideal for studying CO_2 sources and sinks [1][2][3]. This is achieved using the IPDA lidar technique, which relies on much stronger hard target return signals rather than weak atmospheric scattering [4]. In addition, an airborne instrument provides an excellent complement to the temporally-rich but spatially sparse *in-situ* measurement network. The BL weighted XCO2 data can be used to evaluate the ability of GOSAT and OCO-2 to detect spatial variability in lower tropospheric CO_2. Simultaneous airborne measurement of column dry-air volume mixing ratio of H_2O (XH2O) enables the study of coupled carbon and water cycles [4][5][6].

For more than 20 years, researchers at LaRC have developed several high-energy and high repetition rate 2-μm pulsed lasers and other critical components for CO_2 DIAL instruments [7]. The 2-μm wavelength was targeted due to the existence of distinct absorption features for CO_2 at this wavelength region [4]. Currently, LaRC team is engaged in designing, developing and demonstrating a triple-pulsed 2-μm direct detection IPDA lidar to measure XCO2 and XH2O from an airborne platform [4][8][9]. The unique wavelength control for each pulse allows measurement of the two most dominant greenhouse gases, simultaneously and independently, using a single instrument [10]. This work is an update for the 2-μm double-pulse airborne IPDA lidar for CO_2 measurement [11][12]. This paper provides background, status and details of the triple-pulse IPDA development, which enables several technologies for future space-based system for global CO_2 measurement [8].

II. TRIPLE-PULSE IPDA LIDAR TECHNIQUE

Based on the successful demonstration of the double-pulse IPDA lidar, the triple-pulse IPDA lidar transmitter generates three successive laser pulses for every pump pulse [4][11][12]. The pump repetition rate is set to 50 Hz. The three pulses are 150 to 200 μsec apart and set to three different wavelengths, as shown schematically in Fig.1. Using an enhanced wavelength control scheme the wavelength of each of these pulses can be tuned and locked at different wavelength, as marked in Fig.2. One scenario of wavelength selection is demonstrated in the same figure. The CO_2 on and off-line wavelengths are selected around the R30 line, so that both would have similar H_2O absorption to minimizes water vapor interference on CO_2 measurements. Similarly, H_2O on- and off-line are selected around the nearest H_2O absorption peak such that carbon dioxide interference is minimized in the H_2O measurement. However, both CO_2 on-line and H_2O off-line measurements share the same wavelength, which enables simultaneous measurement of both molecules with three pulses rather than four pulses almost independently while avoiding interference from each other [4]. Other different measurement scenarios could be achieved with the same IPDA instrument just by tuning and locking the operating wavelengths of the three pulses to different positions.
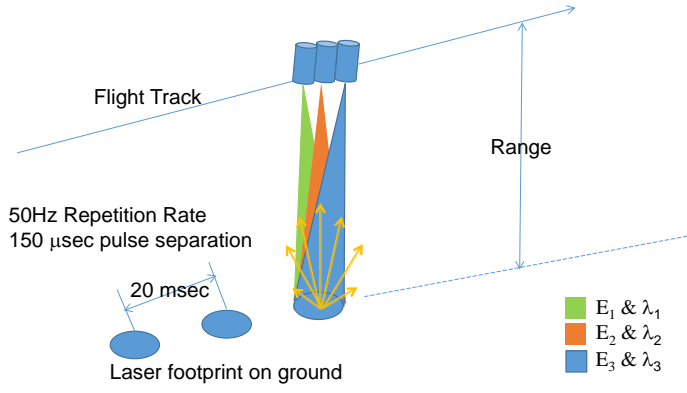
Figure 1. Airborne nadir 2-μm triple-pulse IPDA lidar concept. Each pulse is generated with different wavelength and energy. The three pulses are transmitted every 20 ms, equivalent to 50 Hz repetition rate. Pulse separation of 150-200 ms results in higher than 95% laser footprint overlap above 4 km altitude.

For example, wavelength tuning allows measuring CO_2 with two different weighting functions simultaneously as shown in Fig.3. Fig.3 indicates that the selected CO_2 on-line wavelength is optimized for near-surface measurements. Shifting this wavelength by 67 or 75 pm would tune the weighting function to optimize measurements in the BL or lower troposphere. This tuning feature results in a unique adaptive targeting capability. For an airborne IPDA lidar, adaptive targeting would tune and lock the instrument sensing wavelength to meet certain measurement objective depending on the target or Earth's surface condition and environment. Table 1 lists the double-pulse and triple-pulse 2-μm IPDA lidar transmitter parameters as compared to transmitter requirements for CO_2 space-based active remote sensing. These space-based requirements were set by the European Space Agency (ESA) for a future CO2 active remote sensing mission at the 2-μm wavelength [3][4][12].
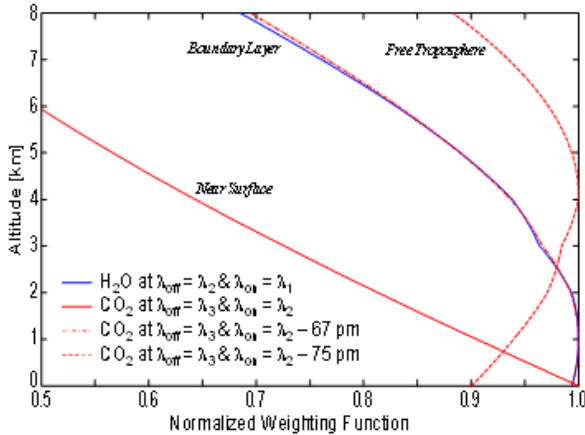

Figure 3. H_2O and CO_2 pressure-based normalized weighting functions versus altitude at selected spectral positions for an airborne nadir pointing IPDA measurement. H_2O and CO_2 measurements are weighted to the boundary layer and near the surface, respectively, for operating wavelength shown in Fig.2. Tuning CO_2 on-line wavelength 67 and 75 pm away from the selected location optimize the IPDA measurement to within the boundary layer or lower troposphere. [4]
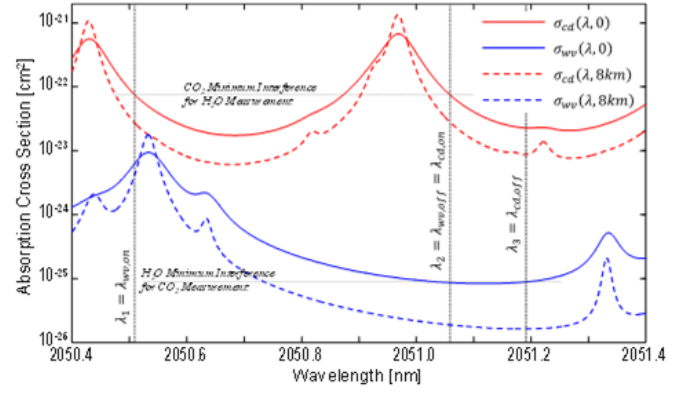

Figure 2. Comparison of the H_2O and CO_2 absorption cross-section spectra, σ_{wv} and σ_{cd}, respectively, at ground (0 km) and mid-altitude aircraft (8 km). Temperature and pressure profiles used in the calculation were obtained from the US Standard atmospheric model. Vertical lines mark the instrument operating wavelengths for CO_2 and H_2O independent measurements. Note that λ_1 is the H_2O on-line, λ_2 serves as the H_2O off-line, and the CO_2 on-line and λ_3 is the CO_2 off-line. The horizontal lines point to minimization of molecular interference errors [4].

III. TRIPLE-PULSE IPDA LIDAR TECHNOLOGY

The 2-μm triple-pulse IPDA lidar consists of a laser transmitter, receiver and data acquisition system. The triple-pulse IPDA laser transmitters is based on the Ho:Tm:YLF high-energy 2-μm pulsed laser technology [7]. The generated 2-μm laser beam is transmitted coaxially with the receiver telescope after beam expansion. Energy monitors, installed inside the laser enclosure, detect and measure the energy of each of the transmitted pulses [11]. The exact wavelengths of the three pulses are controlled by a wavelength control unit.

Table 1. Comparison of CO_2 active remote sensing state-of-the-art 2-μm double-pulse and triple-pulse IPDA laser transmitters, developed at NASA LaRC, with ESA space requirements [4][7].

	Current Technology	Projected Technology	Space Requirement
Transmitter	Single-Laser	Single-Laser	Two Lasers
Technique	Double-Pulse	Triple-Pulse	Single-Pulse
Cooling	Liquid	Conductive	---
Wavelength (μm)	2.051	2.051	2.051
Pulse Energy (mJ)	100 / 50	50 / 15 / 5	40 & 5
Repetition Rate	10 Hz	50 Hz	50 Hz
Power	1.3 W	3.5 W	2.25 W
Pulse Width (ns)	200/350	30/100/150	50
Optical Efficiency	4.0%	5.0%	5.0%
Wall-Plug Efficiency	1.4%	2.1%	>2.0%
Multi-Pulse Delay	200μs	200μs	250±25μs
Transverse Mode	TEM_{00}	TEM_{00}	TEM_{00}
Longitudinal Modes	Single Mode	Single Mode	Single Mode
Pulse Spectral Width	2.2MHz	4-14MHz	> 60MHz
Beam Quality (M^2)	2	2	< 2
Freq. Control Accuracy	0.3 MHz	0.3 MHz	0.2 MHz
Seeding Success Rate	99	99	99
Spectral Purity	99.9%	99.9%	99.9%

A. Triple-Pulse Laser Transmitter

The Ho:Tm:YLF triple-pulse laser is end pumped using 792 nm AlGaAs laser diode arrays. This external pumping targets the Tm, which transfer the stored energy to the Ho relying on the different excitation lifetime. Relative to the pump pulse, Q-switch triggers produces up to three successive laser pulses with relatively controlled energies and pulse-widths. Fig. 4 compares the generated output laser energies for single, double and triple-pulse operation versus the pump laser energy. For three pulse arrangement time separation is approximately 150-200 μs. Thermal analysis was conducted to design proper heat dissipation out of the laser crystal to avoid permanent damage. A prototype oscillator with triple pulsing capability has already been demonstrated. Fig.5 shows a single-shot pulse record generated from the oscillator. Final laser configuration including thermal analysis and alignment optimization is currently on going to achieve higher energies.

B. Wavelength Control

The objective of the wavelength control unit is to provide the required seeding for each of generated pulses. A study indicated that ±1 MHz on-line wavelength jitter is the dominant transmitter systematic error source using this triple-pulse IPDA lidar for CO_2 measurements [4]. This drives the need for a precise wavelength locking mechanism to reduce such error. The exact wavelengths of the pulsed laser transmitter are controlled by the wavelength control unit. The unique wavelength control of the triple pulses uses a single semiconductor laser diode, obtained from NASA Jet Propulsion Laboratory [13] and provides three different seeds of any frequency setting within 35 GHz offset from the locked CO_2 R30 line center reference [10]. This unit includes several electronic, optical and electro-optic components which were acquired and characterized at NASA LaRC. Laser diode driver electronics results in a wavelength jitter of ±6.1 MHz. This jitter is significantly reduced to ±650.1 kHz using center line locking electronics, which meets the jitter limit objective [4]. Fig. 6 shows an optical spectrum analyzer scans for the seeding wavelengths at 6, 16 and 32 GHz offset from the center line locking. Proper filters are included to eliminate harmonics from the generated wavelengths to maintain spectral purity.
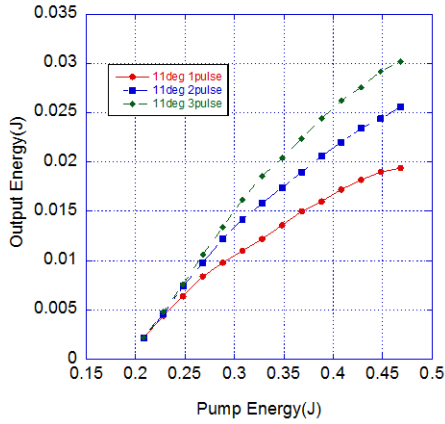

Figure 4. Total output pulse energy versus pump laser energy for the 2-μm IPDA transmitter for single-, double- and triple-pulse operation. Data presented for 50Hz repetition rate and 2.5 ms long pump pulse.

Figure 5. Oscilloscope record for a successful triple-pulse operation of the 2-μm IPDA transmitter. The record shows the profiles of the three pulse (yellow) relative to the Q-switch triggers (red).
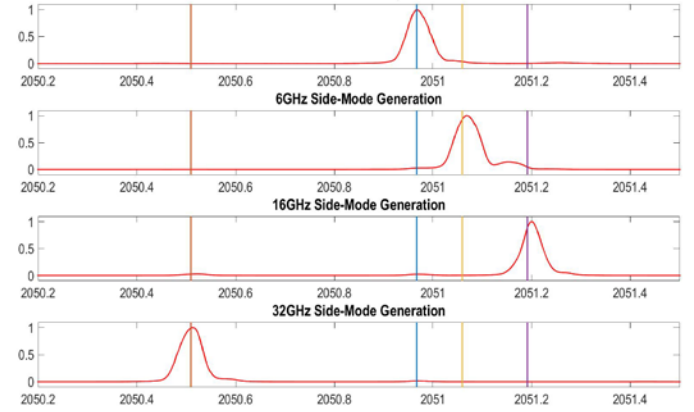

Figure 6. Optical spectrum analyzer scans for the reference wavelength locking to the CO_2 R30 line (top) and the different generated seeding wavelengths for the triple-pulse IPDA transmitter. Vertical lines mark the center line reference (blue), 6 GHz (yellow), 16 GHz (purple) and 32 GHz (orange) spectral positions. Lines are broadened due to the analyzer resolution.

C. IPDA Receiver and Detection Systems

Similar to the double-pulse IPDA, the 2-μm triple-pulse IPDA lidar receiver, shown schematically in Fig. 7, consists of a 0.4 m Newtonian telescope that focuses the radiation onto 300 μm diameter spot. The telescope secondary mirror is a two surface dichroic flat. One surface turns the return radiation 90° to the side integrated aft-optics. The opposite surface is used to transmit the expanded laser beam coaxially with the telescope. A single automated mount is used for bore-sight alignment. The radiation collected by the telescope is focused, collimated, filtered then applied to a 90/10 beam splitter. The 90% signal channel is an exact replica of the double-pulsed lidar using an InGaAs pin photodiode detection system. The 10% channel is planned to be used with an advanced HgCdTe (MCT) electron-initiated avalanche photodiode (e-APD) detection channel. These MCT e-APD devices are space-qualifiable and were validated for airborne lidar operation at 1.6-μm at NASA Goddard Space Flight Center (GSFC) [14]. In co-ordination with NASA Earth Science Technology Office (ESTO), LaRC is collaborating with GSFC to integrate this detector into the 2-μm IPDA. This e-APD exhibit less than 0.5 fW/Hz$^{1/2}$ noise-equivalent-power (NEP) and is expected to enhance the 2-μm
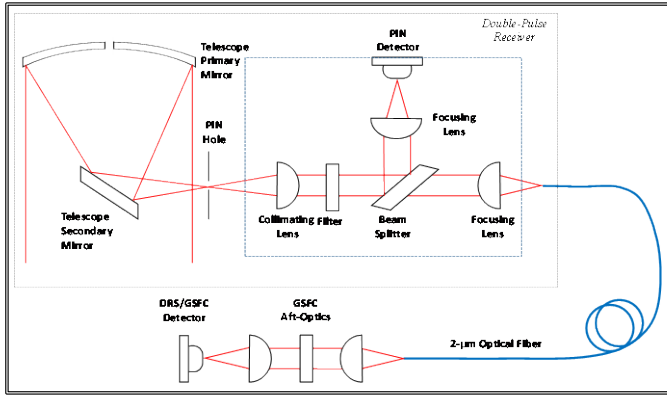
Figure 7. 2-µm triple-pulse IPDA receiver system, integrated based on the previous double-pulse system. The receiver consists of a telescope, aft optics with high-signal InGaAs channel and low-signal e-APD channel. The e-APD channel is coupled through an optical fiber through additional aft-optics.
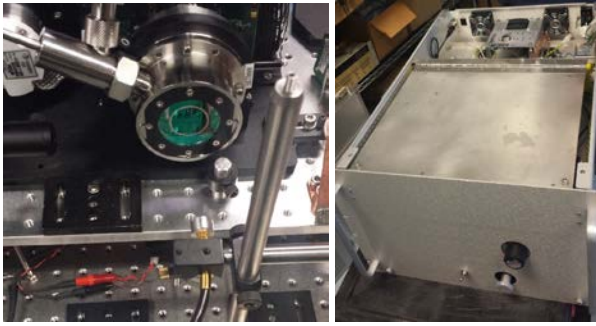

Figure 8. 2-µm triple-pulse IPDA e-APD detection system integrated at NASA GSFC. The e-APD device is cooled inside a vacuum chamber (left), which is integrated inside a rack mountable box (right). The box includes the detector electronics and vacuum circuit for thermal isolation.

IPDA detection performance by expanding the dynamic range and reducing random errors.

MCT e-APD are sensitive to IR radiation up to 4-µm. Therefore, a cold narrow band-pass filter is desired to limit the device background. In co-ordination with ESTO, LaRC collaborated with GSFC to integrate the detector into the triple-pulse 2-µm IPDA lidar. This e-APD comes with 4 by 4 pixel format (80×80 µm² pixel area) with read-out electronics that enable access to each pixel through individual TIA. An output summing amplifier would produce the sum of specific number of pixels as selected by the operator. The detector is integrated inside a vacuum chamber, shown in Fig. 8, which allows cooling the device with cryo-cooler down to 70 K to reduce dark current and noise. The e-APD and readout electronics are integrated inside a rack mountable chassis, shown in the same figure, which includes vacuum circuit for thermal isolation. Additional custom designed aft-optics allows focusing the radiation onto selected number of pixels. The e-APD custom aft-optics is coupled to the IPDA aft-optics through a 2-µm optical fiber, as shown in Fig. 7. Work efforts at GSFC included 2-µm cold filter integration to the detector chamber, detector assembly testing, additional aft-optics design with optical fiber coupling [14][15].

D. IPDA Data Acquisition

The IPDA lidar hard target return signals are digitized and stored using a data acquisition unit. The data acquisition unit is based on two similar high-performance 12-Bit, 1 GS/s digitizers. Each digitizer consists of 2-channels that are enabled through the pump pules and triggered from the laser Q-switch driver. One digitizer is dedicated to the IPDA lidar hard target return signals, with a variable record length to accommodate different operating platform altitudes. The other digitizer is dedicated to laser energy monitors, which are integrated within the transmitter enclosure, with a fixed record length of 10k. Real-time data processing allows visual inspection of measured return signal strengths, optical depths and signal-to-noise ratios. Both raw data and/or processed data storage options are available, which significantly alter storage capacity.

Although, digitized data have 12-bit resolution, data storage is achieved in byte increments, leading to 16-bit data record. This indicates that 25% of the recorded data would be null. Therefore, optional sample averaging take advantage of some of the extra 4-Bits, while enhancing the data record precision, lowering noise and reducing data volume. For example, a 1 second worth of data at 50 Hz repetition rate would results in 150 laser pulses. For each pulse, 4 records are obtained, two from two different energy monitors and another two from the two different detection channels. This would translate to 600 records. Taking into account the record length and two-byte requirement per sample would result in 48 M-Byte/sec data rate. Thus, for an average two hours flight the total data collected would be 344 GByte, at 1 GHz sampling rate. Using sampling average, this can be significantly reduced, while enhancing the noise performance, as demonstrated in figure 9. The figure presents digitizer noise measurements that were conducted with 50Ω floating input for all channels as compared to the ideal quantization noise. Statistical analysis indicated less than 1 mV noise voltage (2 counts at 1 GS/s), which can be reduced further with sample averaging. With 2V input range, this results in signal-to-noise ratio limit of about 2000. Fig. 10 shows an active screen capture for the triple-pulse IPDA data acquisition software graphical user interface (GUI) during ground testing. The figure shows the IPDA operation control as well as horizontal hard target return signals as measured by both the InGaAs pin and e-APD detection channels as compared to the laser energy monitor. In this test, the second energy monitor channel was deactivated.
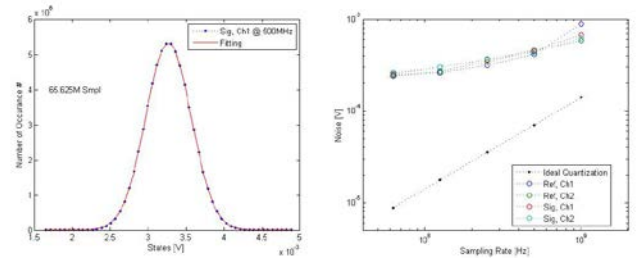

Figure 9. Digitizer noise statistics (left) and noise voltage comparison to ideal quantization error (right). Results indicates less than 1 mV noise voltage (2 counts at 1GS/s), which reduces with sample averaging. With 2V input range, this results in signal-to-noise ratio limit of about 2000.
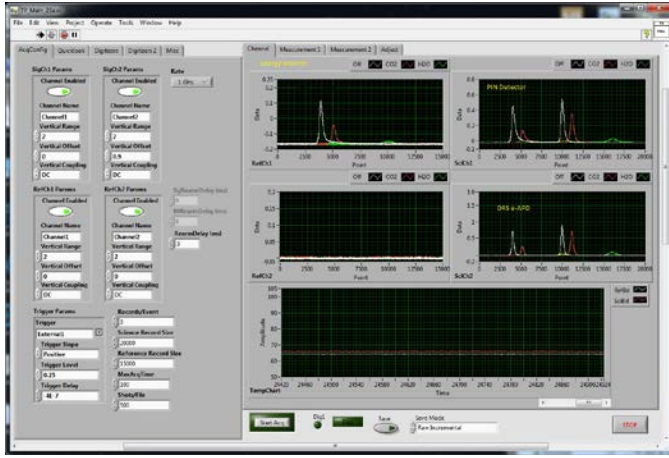
Figure 10. Triple-pulse IPDA lidar data acquisition software GUI showing energy monitor and hard target return signals using InGaAs pin and e-APD detection channels.

IV. INSTRUMNET INTEGRATION AND VALIDATION PLANS

During double-pulse IPDA lidar development, a trailer was prepared as a mobile lidar laboratory for instrument ground testing at NASA LaRC and ground-based field validation campaigns. This trailer will be reused for the triple-pulse IPDA initial integration and ground testing. In addition, availability of the double-pulse instrument provides an excellent test bed for different triple-pulse component evaluation such as, updated laser control electronics, seeding, e-APD detection and data acquisition. Once complete, airborne integration would start by installing the instrument to the NASA B-200 aircraft. The IPDA accommodation inside the aircraft is shown in Fig. 11. The instrument size, weight and power consumption were designed to meet the payload requirements for such small aircraft. This design allows instrument integration to any larger airborne research platform for future missions. Other housekeeping instruments will be integrated into the B-200 aircraft as well, which will include a LiCor *in-situ* sensor for CO_2 and H_2O mixing ratio measurement, Inertial Navigation and Global Positioning Systems (INS/GPS) for global timing, aircraft position, altitude and angles measurements and a video recorder for target identification. Besides, aircraft built-in sensors provide altitude, pressure, temperature and relative humidity sampling at flight position.

The 2-μm triple-pulse IPDA lidar validation is important to assess both CO_2 and H_2O atmospheric measurements. Instrument validation will start during instrument integration in the mobile lidar laboratory. The mobile laboratory enables IPDA lidar horizontal measurement using a set of calibrated hard targets and vertical atmospheric measurements using clouds as hard target. Ground validation objectives are to check the IPDA lidar operational readiness before aircraft deployment. This will be achieved by obtaining IPDA signals and noise to evaluate instrument systematic and random errors, comparing IPDA lidar errors to instrument performance models and to compare with CO_2 and H_2O measurements against correlative *in-situ* instruments. Other objectives include transporting the mobile lidar laboratory, with the integrated instrument, to different tall tower sites, such as WLEF tall tower in Park Falls, Wisconsin, and the Southern Great Plains ARM site in Lamont, Oklahoma.

For airborne validation, initial engineering flights would focus on instrument operation and comparing airborne and ground performances. Later flights would focus on comparing CO_2 and H_2O measurements against correlative *in-situ* sensors and models. Further validation will rely on onboard sensors as well as coordinated measurements with other independent sensors, such as NOAA air-sampling and Pennsylvania State University passive sensors in collaboration with the science community. Airborne validation will be planned to target different conditions such as different surface reflectivity, day and night background, clear, cloudy and broken cloud conditions, variable surface elevation and urban pollution and plume detection. The validation may also cover different locations such as the Upper Midwest summer, where strong vertical and horizontal spatial gradients in atmospheric CO_2 occur due to agricultural activities and urban deployments in winter/summer, with flight around isolated urban centers to identify a clear and polluted boundary layer CO_2 plumes. The 2-μm triple-pulse validation activities provide opportunities to coordinate with ACT-America flights.

V. CONCLUSIONS

A 2-μm double-pulse IPDA lidar instrument have been developed at NASA LaRC. This instrument was validated for active remote sensing of carbon dioxide in the atmosphere. As an upgrade, a 2-μm triple-pulse IPDA lidar instrument is being developed at NASA LaRC. This novel active remote sensing IPDA instrument targets and measures both atmospheric carbon dioxide and water vapor. Wavelength selection and laser transmitter operation allows measuring both species independently and simultaneously. This would be the first demonstration of measuring two different atmospheric molecules with a single instrument. The instrument design is based on knowledge gathered through the previously successful 2-μm double-pulse IPDA. Critical enhancements were implemented in the new triple-pulse design that advances
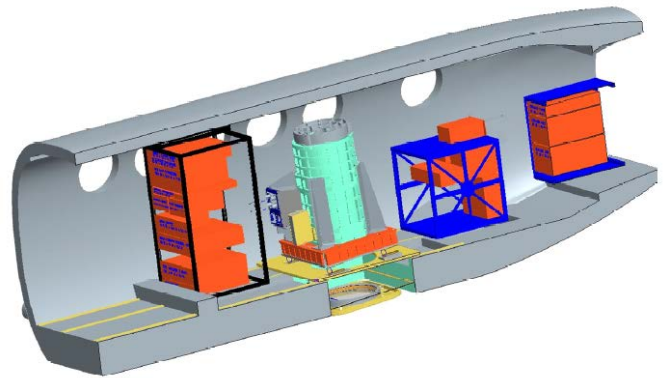

Figure 11. Triple-pulse IPDA lidar anticipated integration onboard the NASA B-200 aircraft. IPDA transmitter and receiver are compactly integrated around the telescope, which is mounted above nadir-view window. IPDA operation and control rack will be populated with necessary electronic for laser timing and control, wavelength control, pump laser driver, data acquisition and diagnostics. A second rack will be dedicated for two-chillers cooling system. A third rack will be reserved for instrumentation backup and *in-situ* measurement.

the technology. These enhancements includes both the transmitter and receiver. For the transmitter, modifications include triple-pulse operation of the laser, laser timing control updates and wavelength control design. In the receiver, updates includes telescope integration, data acquisition system and additional high performance e-APD detector. The e-APD detector supplied by NASA GSFC, is a state-of-art, space qualifiable device that was validated for lidar applications. Combining both the 2-μm triple-pulse transmitter with this new detector in a single instrument will result in a CO_2 IPDA lidar with enabling technology, which meets or exceeds space requirements. Work progress of the 2-μm triple-pulse IPDA program is on schedule. Instrument validation plans are under discussions to collaborate with different institutes with similar interests.

REFERENCES

[1] Active Sensing of CO_2 Emissions over Nights, Days, and Seasons (ASCENDS) Mission, NASA Science Definition and Planning Workshop Report, University of Michigan (2008).

[2] K. Jucks, S. Neeck, J. Abshire, D. Baker, E. Browell, A. Chatterjee, D. Crisp, S. Crowell, S. Denning, D. Hammerling, F. Harrison, J. Hyon, S. Kawa, B. Lin, B. Meadows, R. Menzies, A. Michalak, B. Moore, K. Murray, L. Ott, P. Rayner, O. Rodriguez, A. Schuh, Y. Shiga, G. Spiers, J. Wang, and T. Zaccheo, "Active Sensing of CO_2 Emissions over Nights, Days, and Seasons (ASCENDS) Mission", Science Mission Definition Study (2015).

[3] P. Ingmann, P. Bensi, Y. Duran, A. Griva, and P. Clissold, "A-Scope – advanced space carbon and climate observation of planet earth", ESA Report for Assessment, SP-1313/1 (2008).

[4] T. Refaat, U. Singh, J. Yu, M. Petros, S. Ismail, M. Kavaya, and K. Davis, "Evaluation of an airborne triple-pulsed 2 μm IPDA lidar for simultaneous and independent atmospheric water vapor and carbon dioxide measurements", *Applied Optics*, vol. 54, pp. 1387-1398 (2015).

[5] J. Tadic, M. Loewenstein, C. Frankenberg, L. Iraci, E. Yates, W. Gore and A. Kuze, "A comparison of in-situ aircraft measurements of carbon dioxide to GOSAT data measured over Railroad Valley playa, Nevada, USA", *Atmospheric Measurement Techniques Discussions*, vol. 5, 5641 (2012).

[6] D. Hammerling, A. Michalak and S. Kawa, "Mapping of CO2 at high spatiotemporal resolution using satellite observations: Global distributions from OCO-2", *Journal of Geophysical Research*, vol. 117, D06306 (2012).

[7] U. Singh, B. Walsh, J. Yu, M. Petros, M. Kavaya, T. Refaat, and N. Barnes, "Twenty years of Tm:Ho:YLF and LuLiF laser development for global wind and carbon dioxide active remote sensing", *Optical Materials Express*, vol. 5, pp. 827-837 (2015).

[8] U. Singh, T. Refaat, M. Petros, and J. Yu, "Triple-pulse two-micron integrated path differential absorption lidar: a new active remote sensing capability with path to space", in EPJ Web of Conferences, 27th International Laser Lidar Conference, vol. 119, 02001 (2016).

[9] U. Singh, M. Petros, T. Refaat, and J. Yu, "2-micron triple-pulse integrated path differential absorption lidar development for simultaneous airborne column measurements of carbon dioxide and water vapor in the atmosphere", *Proc. of SPIE*, vol. 9879, 987902, 2016.

[10] T. Refaat, M. Petros, C. Antill, U. Singh, and J. Yu, "Wavelength locking to CO2 absorption line-center for 2-μm pulsed IPDA lidar application", *Proc. SPIE*, vol. 9879, 987904 (2016).

[11] T. Refaat, U. Singh, M. Petros, R. Remus and J. Yu, "Self-calibration and laser energy monitor validation for a double-pulsed 2-μm CO2 integrated path differential absorption lidar application", *Applied Optics*, vol. 54(24), pp. 7240-7251 (2015).

[12] T. Refaat, U. Singh, J. Yu, M. Petros, R. Remus, and S. Ismail, "Double-pulse 2-μm integrated path differential absorption lidar airborne validation for atmospheric carbon dioxide measurement", *Applied Optics*, vol. 55(15), pp. 4232-4246 (2016).

[13] M. Bagheri, G. Spiers, C. Frez, S. Forouhar, and F. Aflatouni, "Linewidth measurement of distributed-feedback semiconductor lasers operating near 2.05 μm," *IEEE Photonics Technology Letters*, vol. 27(18), pp. 1934-1937 (2015).

[14] X. Sun, J. Abshire, and J. Beck, "HgCdTe e-APD detector arrays with single photon sensitivity for space lidar applications", *Proc. SPIE*, vol. 9114, 91140K (2014).

[15] J. Beck, T. Welch, P. Mitra, K. Reiff, X. Sun, and J. Abshire, "A highly sensitive multi-element HgCdTe e-APD detector for IPDA lidar applications", *Journal of Electronic Materials*, vol. 43(8), pp. 2970-2977 (2014).